IEEE Access
Multidisciplinary | Rapid Review | Open Access Journal

Received March 13, 2021, accepted March 23, 2021, date of publication March 29, 2021, date of current version April 6, 2021.

Digital Object Identifier 10.1109/ACCESS.2021.3069328

Shielding Performance of Materials Under the Excitation of High-Intensity Transient Electromagnetic Pulse

ZHIYANG YAN, FENG QIN, JINLIANG CAI, SHOUHONG ZHONG, AND JIANGCHUAN LIN

Institute of Applied Electronics, China Academy of Engineering Physics, Mianyang 621900, China
Key Laboratory of Science and Technology on Complex Electromagnetic Environment, China Academy of Engineering Physics, Mianyang 621900, China

Corresponding author: Feng Qin (fq_soul2000@163.com)

This work was supported in part by the Key Laboratory of Science and Technology on Complex Electromagnetic Environment, China Academy of Engineering Physics (CAEP) under Grant FZSYS-06.

ABSTRACT Shielding effectiveness (SE) dominates the shielding performance of materials. Under the excitation of high-intensity transient electromagnetic pulse, especially the wide-band transient electromagnetic pulse, how to characterize and calculate the SE of shielding materials is not clear. In order to reveal the shielding performance of materials towards the wide-band transient electromagnetic pulse, a systematic experimental investigation was performed on a home-made SE measurement system. The 'peak value reduction (SE_{PR})' is verified to be an effective approach for the characterization of SE of shielding materials. The SE of the employed materials shows no noticeable change even with the excitation field intensity increasing to 200 kV/m, which is significantly different from that of high-power microwave (HPM). Under the excitation of HPM, the SE of materials starts to increase at a field intensity of 19.4 kV/m and becomes saturated at 33.6 kV/m. Further analysis discloses that the variation of SE of materials is mainly dependent on two factors, one is the intrinsic property of the material itself, and the other is energy density spectrum of the excitation high-intensity transient electromagnetic pulse. The energy in per frequency unit (10 MHz) for wide-band transient electromagnetic pulse is far lower than that of HPM, resulting in an evident dissimilarity in the changes of SEs of shielding materials.

INDEX TERMS Shielding performance, wide-band transient electromagnetic pulse, peak value reduction, energy density spectrum.

I. INTRODUCTION

In the past few years, great concern has been paid to the threat brought by high-intensity transient electromagnetic pulse, against the normal working of facilities such as electronic systems, networks, grids and communications [1]–[4], especially with the rapid development of pulsed power science and high-power microwave (HPM) technology [5]–[10]. Improving the survivability of facilities through taking protection and reinforcement measure is crucial for their normal use. Electromagnetic shielding materials, such as carbon-based materials, transition metal oxides/dichalcogenids, silicon carbides and polymer-based composites, which can isolate the sensitive equipment from the electromagnetic radiation in space, have attracted interest of researchers in the field of electromagnetic compatibility, and also show great potential in the reinforcement application against high-intensity transient electromagnetic pulse [11]–[18]. Under the excitation of high-intensity transient electromagnetic pulse, how to characterize the shielding effectiveness (SE) of shielding materials, and whether the shielding performance will be affected by the parameters such as field intensity, repetition frequency and pulse width are thus very critical for practical applications.

Presently, the characterization and description of SE for shielding materials are clear under the excitation of continuous small signal [19]–[21]. As to high-intensity transient electromagnetic pulse, related work mainly focus on theoretic analysis, numerical simulation and experimental investigation based on standard waveforms such as Gauss pulse, double exponential pulse and square pulse [22]–[30]. Till very recently, a comprehensive study on the shielding performance of materials under the excitation of HPM was conducted [31], and Per Ängskog *et al.* [32] reported a detailed investigation on the SE and HPM vulnerability of energy-saving windows and window panes. However, almost no work has

The associate editor coordinating the review of this manuscript and approving it for publication was Guangcun Shan.

been made on how to characterize the SE of materials under the excitation of wide-band transient electromagnetic pulse and whether the shielding performance will be affected by the pulse parameters is unclear.

The aim of this work is to clarify the characterization of SE of materials against wide-band transient electromagnetic pulse and reveal the underlying mechanism that affects the SE of materials under the excitation of high-intensity transient electromagnetic pulse. The 'peak value reduction (SE_{PR})' is approved to be a suitable approach for the characterization of SE of materials. The SE of materials exhibits no noticeable variation even with the excitation field intensity of wide-band transient electromagnetic pulse reaching 200 kV/m, which is greatly different from that of HPM. Under the excitation of HPM, the SE of materials first keeps unchanged, then starts to increase, and finally saturates with the increment of field intensity. Further analysis reveals that the variation of SE of materials is mainly dependent on two factors, one is the intrinsic property of the material itself, and the other is energy density spectrum of high-intensity transient electromagnetic pulse. The energy in per frequency unit (10 MHz) for wide-band transient electromagnetic pulse is far less than that of HPM, which leads to a distinctly different evolution of the SE of shielding materials.

II. EXPERIMENTAL METHOD

A. EXPERIMENTAL SYSTEM

The experiments were performed on a home-made SE measurement system, as shown in Fig. 1(a). A wide-band transient electromagnetic pulse radiation device with rE (field-intensity distance product on the main beam axis) of 300 kV is employed as the excitation source. A test box with a 600 mm × 600 mm test window is placed in the microwave anechoic chamber. The field intensity is adjusted by changing the distance between the wide-band transient electromagnetic pulse source and test box. As a result, field intensities in the range of 10–200 kV/m are easily obtained. Four different kinds of shielding materials, such as Ag doped shielding filling, Ag-Cu doped shielding filling, Cu-mesh embedded shielding glass and ITO coated shielding glass, were purchased from 33rd Research Institute of China Electronics Technology Group Corporation (CETC 33), Taiyuan, China and were cut into 640 mm × 640 mm that can well match the window size of the measurement system. All of the four shielding materials are rigid, not having good flexibility. The SEs of them are not dependent on frequency in the frequency regime of 100 MHz to 8 GHz under the excitation of continuous small signal, which are probably owing to the component and structure of materials employed. A typical output waveform of the wide-band transient electromagnetic pulse source is shown as Fig. 1(b). It is clear to see that the excitation pulse lasts for about 10 ns. Fast Fourier Transform (FFT) was then performed to obtain its amplitude-frequency characteristics (Fig. 1(c)). The excitation pulse signal has a central frequency of about 380 MHz, and its -10-dB bandwidth is in the range from 200 to 500 MHz.

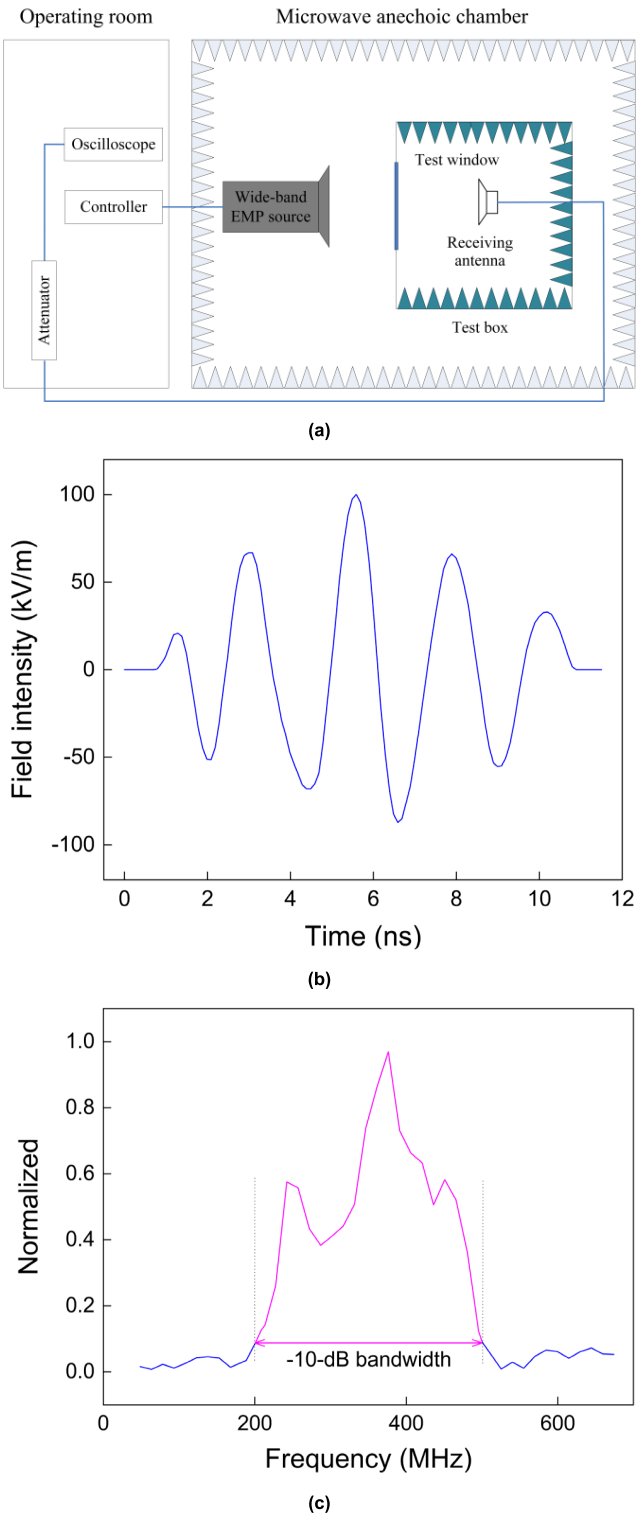

FIGURE 1. (a) Schematic illustrating the SE measurement system for wide-band transient electromagnetic pulse. (b) Typical time-domain output waveform of the wide-band transient electromagnetic pulse source. (c) Corresponding normalized amplitude-frequency curve of the output waveform.

B. SHIELDING EFFECTIVENESS

SE is defined as the logarithm ratio of the voltage or power obtained by the receiving antenna without/with a shielding

material on the window of the test device [19]–[21].

$$SE = 20\log\frac{V_1}{V_2} \tag{1}$$

$$SE = 10\log\frac{W_1}{W_2} \tag{2}$$

V_1 and W_1 are the received voltage and energy when the shielding material is not placed on the test window, respectively. V_2 and W_2 correspond to the received voltage and energy once the shielding material is positioned on the test window.

In the experimental system, the signal receiving loop consists of a wide-band receiving antenna inside the test box, a transmission cable, attenuators with suitable power capacity and a digital oscilloscope. By changing the attenuation value of the attenuator, the receiving signal can be well displayed by the oscilloscope. Supposing R_a and R_c the attenuation (in dB) of the attenuator and transmission cable, respectively, as well as V_p the peak voltage of the time-domain waveform recorded by the oscilloscope, the field intensity (E) of the wide-band transient electromagnetic pulse received by the receiving antenna can thus be expressed as

$$E = \frac{V_p 10^{(R_a+R_c)/20}}{h_e} \tag{3}$$

h_e donates the effective height of the receiving antenna.

As a result, SE of the shielding materials calculated by peak value reduction (SE_{PR}) can be described as

$$SE_{PR} = 20\log\frac{E_1}{E_2} = 20\log\frac{V_{p,1}10^{\frac{(R_{a,1}+R_c)}{20}}\Big/h_e}{V_{P,2}10^{\frac{(R_{a,2}+R_c)}{20}}\Big/h_e}$$

$$= 20\log\frac{V_{p,1}}{V_{p,2}} + R_{a,1} - R_{a,2} \tag{4}$$

$V_{p,1}$ and $R_{a,1}$ are the peak voltage and attenuation when the shielding material is not present on the test window, respectively. $V_{p,2}$ and $R_{a,2}$ represent the peak voltage and attenuation as the shielding material is placed on the test window.

The frequency-domain SE (SE_{FD}) can be calculated based on the amplitude-frequency curve and path attenuation before and after the shielding material is present on the test window.

$$SE_{FD} = 20\log\frac{V_{f,1}}{V_{f,2}} + R_{a,1} - R_{a,2} \tag{5}$$

$V_{f,1}$ and $V_{f,2}$ represent the voltage at a specific frequency without/with the shielding material on the test window.

The gain of the receiving antenna depends on the efficiency factor k and directivity D, which can be expressed as

$$G = kD \tag{6}$$

D is equal to the ratio of the maximum power density to its average value over a sphere as observed in the far field of an antenna, which can be written as

$$D = 4\pi\frac{A_e}{\lambda^2} \tag{7}$$

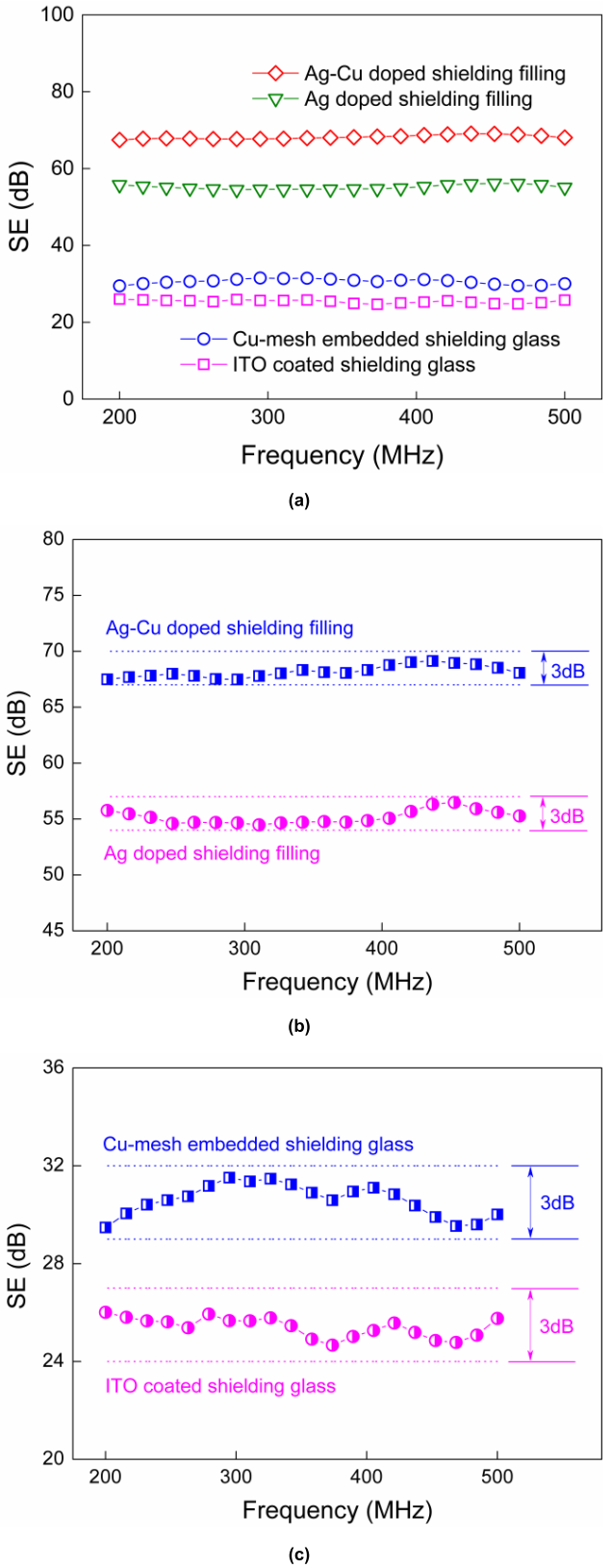

FIGURE 2. Frequency-domain SEs of four different kinds of shielding materials.

A_e denotes the effective aperture of the receiving antenna and can be given as

$$A_e = \frac{h_e^2 Z_0}{4R_r} \tag{8}$$

Z_0 and R_r are the intrinsic impedance of free space and radiation resistance of the receiving antenna, respectively.

According to (6), (7) and (8), the gain of the receiving antenna can be calculated as

$$G = h_e^2 \frac{k\pi Z_0}{\lambda^2 R_r} \tag{9}$$

For the time-domain signal of wide-band transient electromagnetic pulse acquired by the oscilloscope, its energy can be calculated as

$$W_o = \int_T \frac{V(t)^2}{R} dt \tag{10}$$

T represents the duration of the transient signal, R denotes the characteristic impedance of the receiving loop and $V(t)$ is the voltage component of the time-domain waveform.

Taking into consideration of the energy calculated by the time-domain signal of wide-band transient electromagnetic pulse recorded by the oscilloscope, the path attenuation and the gain of antenna, the energy received by the antenna can be calculated as

$$\begin{aligned} W &= 10^{G/10} W_o^{(R_a+R_c)/10} \\ &= 10^{h_e^2 k\pi Z_0/10\lambda^2 R_r} W_o^{(R_a+R_c)/10} \\ &= 10^{h_e^2 k\pi Z_0/10\lambda^2 R_r} \left[\int_T \frac{V(t)^2}{R} dt\right]^{(R_a+R_c)/10} \end{aligned} \tag{11}$$

As a result, the energy reduction SE can be calculated as, (12) shown at the bottom of the page.

III. CHARACTERIZATION OF SHIELDING EFFECTIVENESS

Fig. 2(a) shows the frequency-domain SEs of the four kinds of shielding materials under the excitation of wide-band transient electromagnetic pulse with a field intensity of 20 kV/m. It is apparent that the SEs keep almost unchanged in the frequency range from 200 MHz to 500 MHz. Further analysis shows the fluctuation in the SEs is very slight, not exceeding 3 dB in the entire frequency regime (Fig. 2(b) and Fig. 2(c)). Taking into consideration of the measurement errors and intrinsic characteristics of wide-band transient electromagnetic pulse, a 3-dB fluctuation in measured SEs can be ignored. The SE_{FD} of these four shielding materials can thus be approximately characterized by using the SE

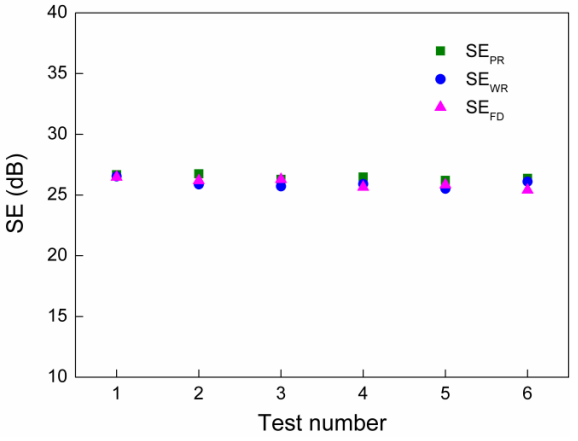

FIGURE 3. SE_{PR}, SE_{WR} and SE_{FD} of ITO coated shielding glass.

of the central frequency (380 MHz). Fig. 3 shows the SEs of ITO coated shielding glass calculated by the 'peak value reduction', 'frequency-domain SE based on FFT' and 'energy reduction'. We can clearly see that the SEs calculated by different methods are nearly the same. The difference in between them is so slight that it can be ignored.

The SEs of these four kinds of shielding materials under the excitation of wide-band transient electromagnetic pulse are displayed in Table 1. It is evident that for all the four shielding materials employed in our experiments, the percentage of maximum deviation at absolute value of SE calculated by 'frequency domain SE based on FFT' and 'energy reduction' does not exceed 1.76% and 2.12%, respectively, in comparison with that obtained by using 'peak value reduction' method. Such phenomenon is probably ascribed to the insensitivity of the SE on frequency within the main frequency regime of wide-band transient electromagnetic pulse. Considering that the peak value of the time-domain signal can be directly obtained from the waveform acquired by oscilloscope, so 'peak value reduction' characterization can be employed as a simple and convenient way to calculate the SE of shielding materials under the excitation of wide-band transient electromagnetic pulse.

IV. SHIELDING PERFORMANCE UNDER THE EXCITATION OF HIGH-INTENSITY TRANSIENT ELECTROMAGNETIC PULSE

For high-intensity transient electromagnetic pulse, it is often considered that the parameters such as repetition frequency,

$$\begin{aligned} SE_{WR} &= 10\lg\frac{W_1}{W_2} \\ &= 10\lg\left\{10^{h_e^2 k\pi Z_0/10\lambda^2 R_r}\left[\int_T \frac{V_1(t)^2}{R} dt\right]^{(R_{a,1}+R_c)/10}\right\} \Bigg/ \left\{10^{h_e^2 k\pi Z_0/10\lambda^2 R_r}\left[\int_T \frac{V_2(t)^2}{R} dt\right]^{(R_{a,2}+R_c)/10}\right\} \\ &= 10\lg\left[\int_T \frac{V_1(t)^2}{R} dt \Bigg/ \int_T \frac{V_2(t)^2}{R} dt\right] + \left(R_{a,1} - R_{a,2}\right) \end{aligned} \tag{12}$$

field intensity and pulse width play an important role in the electromagnetic interference effect on electronic systems [33]–[35]. Whether the shielding performance of materials will be affected by the parameters of high-intensity transient electromagnetic pulse is crucial for their practical applications. In a piece of previous work [31], a comprehensive investigation about shielding performance of materials under the excitation of HPM has been performed. It has been found that with the increase of the power density ($\sim E^2/377$) of HPM, the SE of materials first keeps unchanged, then increases and finally saturates, and other parameters like repetition frequency and pulse width of HPM have a negligible effect on the shielding performance of materials.

In order to have a comprehensive understanding of various parameters of wide-band transient electromagnetic pulse on the shielding performance of materials, a systematic investigation was carried out. Fig. 4 shows the measured SEs of the four kinds of shielding materials with different repetition frequency and field intensity. When the field intensity of the wide-band transient electromagnetic pulse is 20 kV/m, the SEs keep almost unvaried with the repetition frequency in the range of 1–50 Hz (Fig. 4(a)). Similarly, with the variation of field intensity from 1 to 200 kV/m, SEs of shielding materials under the excitation of wide-band transient electromagnetic pulse with repetition frequency of 1 Hz are nearly unchanged (Fig. 4(b)).

Comparative SE measurements were further performed on these four kinds of shielding materials with the excitation of HPM. The experimental setup for HPM SE measurements has been well introduced in an article published by us recently [31]. An L-band klystron microwave power amplifier with carrier frequency of 1.35 GHz is employed as the HPM source, and the excitation field intensity can be easily tuned in the range from 6.1 to 43.4 kV/m. No noticeable change in SEs can be observed for the Cu-mesh embedded shielding glass and ITO coated shielding glass even for the field intensity is increased to 43.4 kV/m (Fig. 5(a)). In contrast, the shielding performances of the Ag-Cu doped shielding filling and Ag doped shielding filling are obviously affected by the radiation of HPM. When the field intensity reaches nearly 19.4 kV/m, the SEs of these two materials tend to become larger. Hereafter, with the continuous increment of field intensity, the SE is increased from nearly 70 dB/57 dB to 78 dB/64 dB for Ag-Cu doped shielding filling and Ag doped shielding filling, respectively. As the field intensity attains approximately 33.6 kV/m, the SEs of the two materials become saturated. Further increase in the field intensity doesn't give rise to improvement of the SEs (Fig. 5(b)).

Under the excitation of HPM, microscopic interconnections produced by polarization or thermal effect in Ag-Cu doped shielding filling and Ag doped shielding filling can improve their electrical conductivities, which in turn lead to the increase of the SEs. Once the field intensity is increased to a certain value, the polarization or thermal effect induced interconnection saturates and the electrical conductivity no longer gets larger. As a result, the SEs of these two kinds of

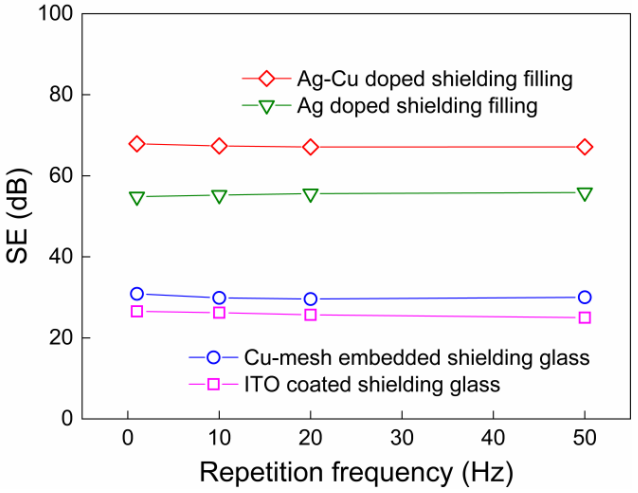

(a)

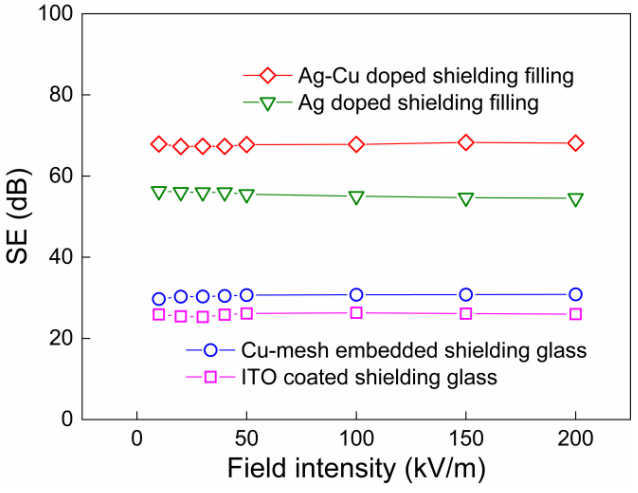

(b)

FIGURE 4. SEs of four kinds of shielding materials under the excitation of wide-band transient electromagnetic pulse with different (a) repetition frequency and (b) field intensity.

TABLE 1. Percentage of maximum deviation at absolute value of four groups of materials.

Material	Percentage of maximum deviation at absolute value	
	$\lvert SE_{WR}\text{-}SE_{PR}\rvert/SE_{PR}$	$\lvert SE_{FD}\text{-}SE_{PR}\rvert/SE_{PR}$
Ag-Cu doped shielding filling	1.72%	1.76%
Ag doped shielding filling	2.12%	1.56%
Cu-mesh embedded shielding glass	1.03%	0.96%
ITO coated shielding glass	1.25%	1.01%

shielding materials become saturated. Contrarily, for the other two shielding materials like Cu-mesh embedded shielding glass and ITO coated shielding glass, it is probably owing to that no obvious microscopic interconnection is produced under the excitation of HPM with field intensity in the range of 6.1-43.4 kV/m.

It is worth noting that with the increase of field intensity, Ag-Cu doped shielding filling and Ag doped shielding filling exhibit completely different shielding performances against

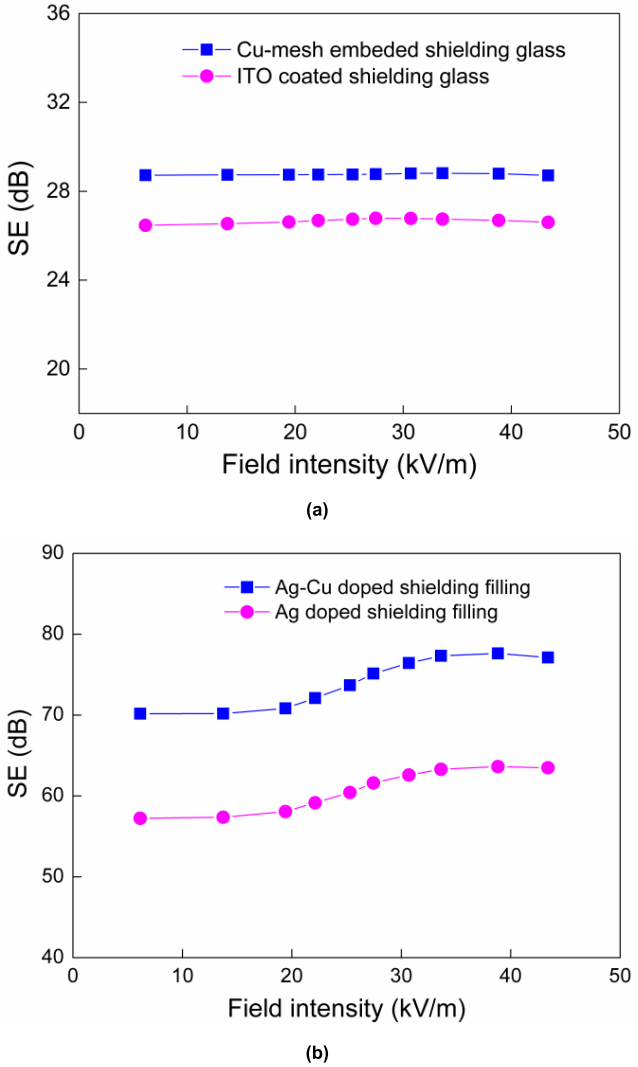

FIGURE 5. SEs of (a) Cu-mesh embedded shielding glass, ITO coated shielding glass and (b) Ag-Cu doped shielding filling, Ag doped shielding filling under the excitation of HPM with different field intensity.

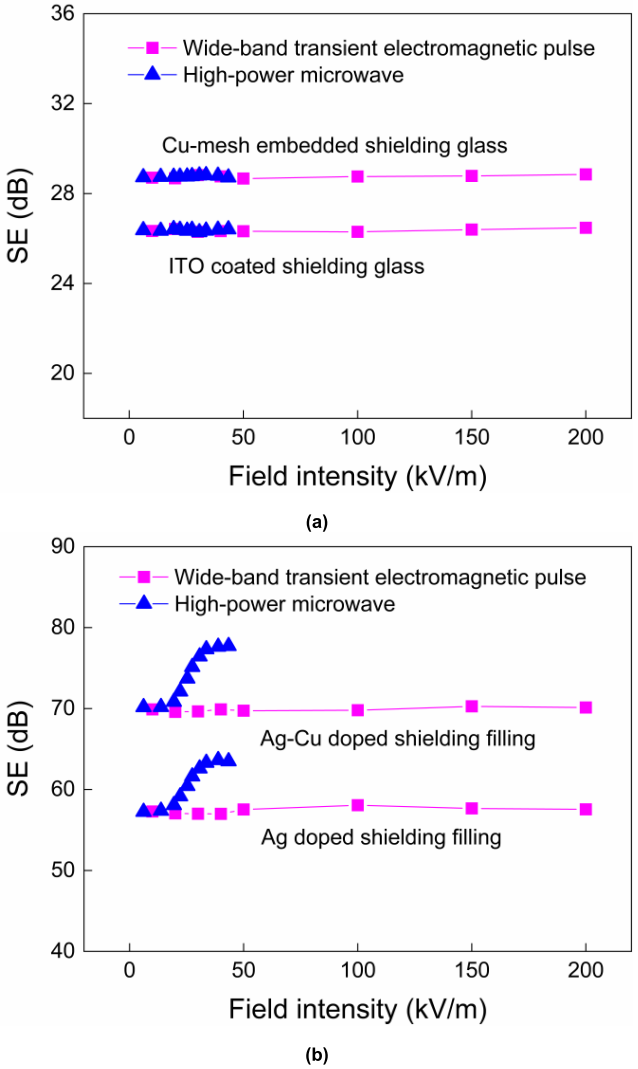

FIGURE 6. Evolutions of SEs with the field intensities of wide-band transient electromagnetic pulse and HPM. (a) shielding filling, (b) shielding glass.

wide-band transient electromagnetic pulse and HPM. The SE keeps unchanged even with the field intensity increasing to 200 kV/m for wide-band transient electromagnetic pulse, whereas for HPM, the SE is continuously increased with the field intensity in the range from 19.4 to 33.6 kV/m. Since the frequency regime of wide-band transient electromagnetic pulse is different from that of HPM, the influence of frequency on SE was thus investigated. As shown in Fig. 6 (a), the SEs of Cu-mesh embedded shielding glass and ITO coated shielding glass are measured to be ∼29 dB and ∼26 dB under these two excitations, respectively, indicating the frequency almost has no effect on the SEs. For Ag-Cu doped shielding filling and Ag doped shielding filling, it is clearly observed that before the SEs start to increase under the excitation of HPM, the SEs are nearly maintained at 70 dB and 57 dB (Fig. 6(b)), which further demonstrates that the frequency has ignorable influence on the SEs. Fig. 7(a) shows the normalized amplitude-frequency curve of HPM, from which we can clearly see that the central frequency of HPM locates at 1350 MHz and the −10-dB bandwidth ranges from nearly 1345 MHz to 1355 MHz, which differs significantly from that (200–500 MHz) of wide-band transient electromagnetic pulse (Fig. 1(c)). For HPM signal with a field intensity of 19.4 kV/m, the energy distributed in per frequency unit (10 MHz), i.e., energy spectrum density, is 0.1746 J/10 MHz (Fig. 7(b)). As to wide-band transient electromagnetic pulse, the maximum energy spectrum density doesn't exceed 0.0189 J/10 MHz even with the field intensity of 200 kV/m (Fig. 7(c)). The maximum energy spectrum density of wide-band transient electromagnetic pulse is far less than that of HPM, which is probably the reason why no improvement in the SEs of shielding materials is observed under the excitation of wide-band transient electromagnetic pulse. As a result, the SEs of shielding materials exhibit distinctly different evolution phenomena for wide-band transient electromagnetic pulse and HPM. Based on aforementioned

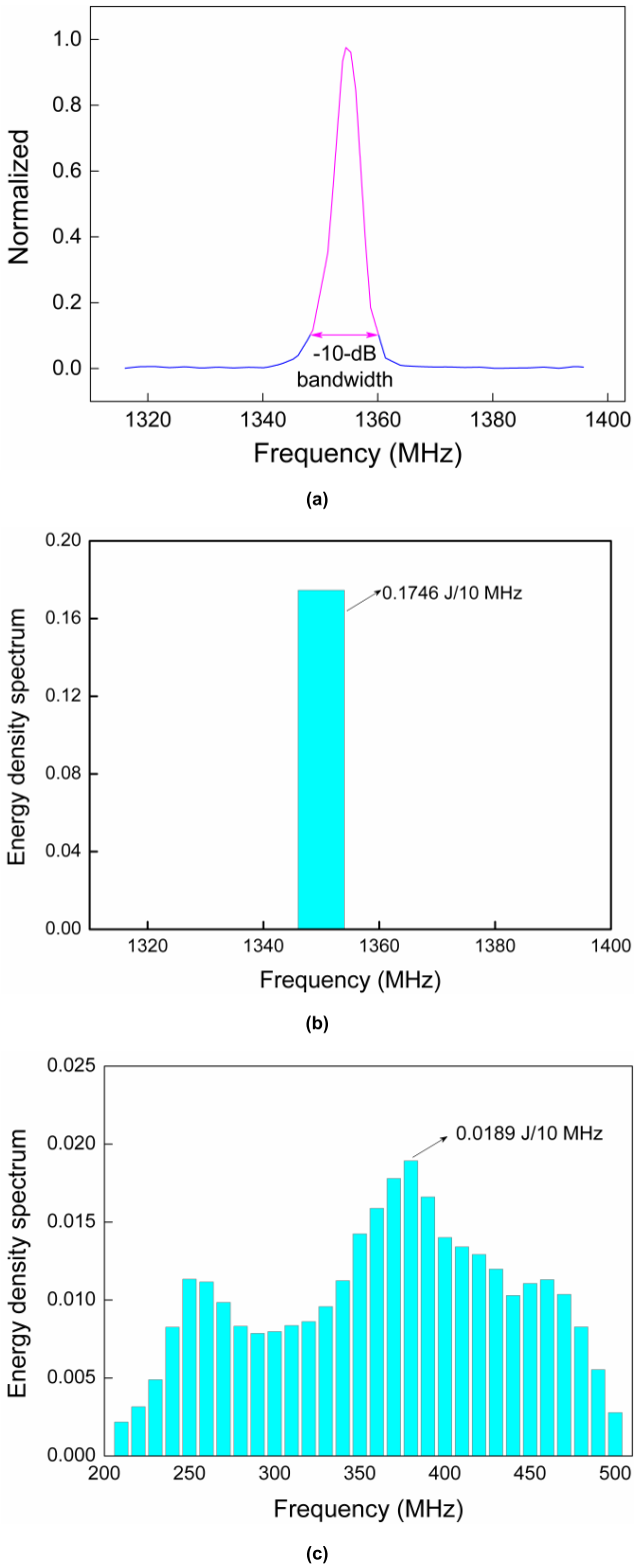

FIGURE 7. **(a) Normalized amplitude-frequency characteristics of HPM signal. (b, c) Energy density spectrum of HPM and wide-band transient electromagnetic pulse, respectively.**

results, we put forward a hypothesis here if the excitation field intensity of wide-band transient electromagnetic pulse attains a value of approximate 608 kV/m, a phenomenon that the SE of shielding materials starts to increase should appear.

V. CONCLUSION

Under the excitation of wide-band transient electromagnetic pulse, the 'peak value reduction (SE_{PR})' can be employed to characterize the SE of shielding materials. The SE of the shielding materials exhibits no noticeable change even with the excitation field intensity reaching 200 kV/m, which is greatly different from that of HPM. Under the excitation of HPM, the SE of materials starts to increase at a field intensity of 19.4 kV/m and saturates at 33.6 kV/m. Further analysis reveals that the variation of SE of shielding materials is mainly determined by two factors, one is the intrinsic property of the material itself, and the other is energy density spectrum of the excitation high-intensity transient electromagnetic pulse. The energy in per frequency unit (10 MHz) for wide-band transient electromagnetic pulse is far less than that of HPM, leading to a distinctly different evolution of the SEs of shielding materials.

ACKNOWLEDGMENT

(Zhiyang Yan and Feng Qin are co-first authors.)

REFERENCES

[1] W. A. Radasky, C. E. Baum, and M. W. Wik, "Introduction to the special issue on high-power electromagnetics (HPEM) and intentional electromagnetic interference (IEMI)," *IEEE Trans. Electromagn. Compat.*, vol. 46, no. 3, pp. 314–321, Aug. 2004.

[2] R. Przesmycki, "Classification of the electromagnetic effects of information devices during high power microwave exposing," in *Proc. Prog. Electromagn. Res. Symp. (PIERS-FALL)*, Singapore, Nov. 2017, pp. 357–363.

[3] F. Brauer, F. Sabath, and J. L. ter Haseborg, "Susceptibility of IT network systems to interferences by HPEM," in *Proc. IEEE Int. Symp. Electromagn. Compat.*, Austin, TX, USA, Aug. 2009, pp. 237–242.

[4] M. Lanzreth, M. Suhrke, and H. Hirsch, "HPEM vulnerability of smart substation secondary systems," in *Proc. Int. Symp. Electromagn. Compat.*, Amsterdam, The Netherlands, Aug. 2018, pp. 799–804.

[5] M. Gundersen, P. T. Vernier, S. B. Cronin, and S. Kerketta, "A review of diverse academic research in nanosecond pulsed power and plasma science," *IEEE Trans. Plasma Sci.*, vol. 48, no. 4, pp. 742–748, Apr. 2020.

[6] J. Deng *et al.*, "Overview of pulsed power research at CAEP," *IEEE Trans. Plasma Sci.*, vol. 43, no. 8, pp. 2760–2765, Aug. 2015.

[7] F. Hamamah, W. F. H. W. Ahmad, C. Gomes, M. M. Isa, and M. J. Homam, "High power microwave devices: Development since 1880," in *Proc. IEEE Asia–Pacific Microw. Conf. (APMC)*, Kuala Lumpar, Malaysia, Nov. 2017, pp. 825–828.

[8] W. D. Prather, C. E. Baum, R. J. Torres, F. Sabath, and D. Nitsch, "Survey of worldwide high-power wideband capabilities," *IEEE Trans. Electromagn. Compat.*, vol. 46, no. 3, pp. 335–344, Aug. 2004.

[9] F. Sabath, M. Bäckström, B. Nordström, D. Sérefin, B. A. Kerr, and D. Nitsch, "Overview of four European high-power microwave narrowband test facilities," *IEEE Trans. Electromagn. Compat.*, vol. 46, no. 3, pp. 329–334, Aug. 2004.

[10] N. S. Kushwaha and M. M. Sharma, "High power microwave technology and its military implications," in *Proc. Int. Conf. Recent Adv. Microw. Theory Appl.*, Jaipur, India, Nov. 2008, pp. 871–874.

[11] S. Geetha, K. K. Satheesh, C. R. K. Rao, M. Vijayan, and D. C. Trivedi, "EMI shielding: Methods and materials—A review," *J. Appl. Polym. Sci.*, vol. 112, no. 4, pp. 2073–2086, May 2009.

[12] C. Wang, V. Murugadoss, J. Kong, Z. He, X. Mai, Q. Shao, Y. Chen, L. Guo, C. Liu, S. Angaiah, and Z. Guo, "Overview of carbon nanostructures and nanocomposites for electromagnetic wave shielding," *Carbon*, vol. 140, pp. 696–733, Dec. 2018.

[13] D. Jiang, V. Murugadoss, Y. Wang, J. Lin, T. Ding, Z. Wang, Q. Shao, C. Wang, H. Liu, N. Lu, R. Wei, A. Subramania, and Z. Guo, "Electromagnetic interference shielding polymers and nanocomposites—A review," *Polym. Rev.*, vol. 59, no. 2, pp. 280–337, Feb. 2019.

[14] M. Cao, X. Wang, M. Zhang, J. Shu, W. Cao, H. Yang, X. Fang, and J. Yuan, "Electromagnetic response and energy conversion for functions and devices in low-dimensional materials," *Adv. Funct. Mater.*, vol. 29, no. 25, Jun. 2019, Art. no. 1807398.
[15] O. Balci, E. O. Polat, N. Kakenov, and C. Kocabas, "Graphene-enabled electrically switchable radar-absorbing surfaces," *Nature Commun.*, vol. 6, no. 1, p. 6628, Mar. 2015.
[16] B. Wen, M. S. Cao, M. M. Lu, W. Q. Cao, H. L. Shi, J. Liu, X. X. Wang, H. B. Jin, X. Y. Fang, W. Z. Wang, and J. Yuan, "Reduced graphene oxides: Light-weight and high-efficiency electromagnetic interference shielding at elevated temperatures," *Adv. Mater.*, vol. 26, no. 21, pp. 3484–3489, Jun. 2014.
[17] M. Hu, N. Zhang, G. Shan, J. Gao, J. Liu, and R. K. Y. Li, "Two-dimensional materials: Emerging toolkit for construction of ultrathin high-efficiency microwave shield and absorber," *Frontiers Phys.*, vol. 13, no. 4, Jul. 2018, Art. no. 138113.
[18] D. Zhang, H. Wang, J. Cheng, C. Han, X. Yang, J. Xu, G. Shan, G. Zheng, and M. Cao, "Conductive WS2-NS/CNTs hybrids based 3D ultra-thin mesh electromagnetic wave absorbers with excellent absorption performance," *Appl. Surf. Sci.*, vol. 528, Oct. 2020, Art. no. 147052.
[19] *Method of Attenuation Measurements for Enclosures, Electromagnetic Shielding, for Electronic Test Purpose*, Standard MIL-STD-285, 1956.
[20] *IEEE Standard Method for Measurig the Effectiveness of Electromagnetic Shielding Enclosures*, IEEE Standard 299, 1997.
[21] *Standard Test Method for Measuring the Electromagnetic Shielding Effectiveness of Planar Materials*, Standard ASTM D4935, 2010.
[22] L. Klinkenbusch, "On the shielding effectiveness of enclosures," *IEEE Trans. Electromagn. Compat.*, vol. 47, no. 3, pp. 589–601, Aug. 2005.
[23] J. Zou, J. Guo, J. L. He, S. J. Han, R. Zeng, and X. S. Ma, "Evaluation of the EMP shielding effectiveness for the thin metallic shells," in *Proc. Asia–Pacific Conf. Environ. Electromagn.*, Hangzhou, China, Nov. 2003, pp. 410–413.
[24] L. Zhang, X. Hu, X. Lu, G. Zhu, and Y. Zhang, "Simulation analysis for the materials shielding effectiveness of EMP," in *Proc. Cross Strait Quad-Regional Radio Sci. Wireless Technol. Conf.*, Harbin, China, Jul. 2011, pp. 32–35.
[25] S.-Y. Hyun, K.-W. Lee, and J.-G. Yook, "Modeling of shielding effectiveness of reinforced concrete walls for electromagnetic pulse," in *Proc. 42nd Eur. Microw. Conf.*, Amsterdam, The Netherlands, Oct. 2012, pp. 453–456.
[26] X.-F. Hu, X. Chen, and M. Wei, "Time-domain simulation and waveform reconstruction for shielding effectiveness of materials against electromagnetic pulse," *J. Phys., Conf. Ser.*, vol. 418, Mar. 2013, Art. no. 012011.
[27] S. Celozzi and R. Araneo, "Alternative definitions for the time-domain shielding effectiveness of enclosures," *IEEE Trans. Electromagn. Compat.*, vol. 56, no. 2, pp. 482–485, Apr. 2014.
[28] P. Chen, C. Mao, and G. Wu, "Shielding effectiveness assessment of enclosure by means of EMP excitation," in *Proc. Asia–Pacific Int. Symp. Electromagn. Compat. (APEMC)*, Shenzhen, China, May 2016, pp. 273–275.
[29] Z. Bihua, G. Cheng, and R. Heming, "The definition of EMP shielding effectiveness," in *Proc. Asia–Pacific Conf. Environ. Electromagn.*, Hangzhou, China, Nov. 2003, pp. 562–565.
[30] X. Chen, Y. G. Chen, M. Wei, and M. Cui, "Broadband coaxial holder with continuous-conductor used for shielding effectiveness of materials against electromagnetic pulse," *Electron. Lett.*, vol. 49, no. 8, pp. 532–534, Apr. 2013.
[31] Z. Yan, F. Qin, and J. Cai, "Shielding effectiveness of materials under the excitation of high-power microwave," *IEEE Trans. Electromagn. Compat.*, vol. 62, no. 5, pp. 2317–2320, Oct. 2020.
[32] P. Ängskog, M. Bäckström, C. Samuelsson, and B. K. Vallhage, "Shielding effectiveness and HPM vulnerability of energy-saving windows and window panes," *IEEE Trans. Electromagn. Compat.*, vol. 61, no. 3, pp. 870–877, Jun. 2019.
[33] M. G. Bäckström and K. G. Lövstrand, "Susceptibility of electronic systems to high-power microwaves: Summary of test experience," *IEEE Trans. Electromagn. Compat.*, vol. 46, no. 3, pp. 396–403, Aug. 2004.
[34] C. Kou, X. Tang, K. Shao, and J. Liu, "High power microwave interference effect of radar system," in *Proc. IEEE 4th Adv. Inf. Technol., Electron. Autom. Control Conf. (IAEAC)*, Chengdu, China, Dec. 2019, pp. 422–427.
[35] D. MÅnsson, R. Thottappillil, T. Nilsson, O. Lundén, and M. Bäckström, "Susceptibility of civilian GPS receivers to electromagnetic radiation," *IEEE Trans. Electromagn. Compat.*, vol. 50, no. 2, pp. 434–437, May 2008.

ZHIYANG YAN was born in Meishan, China, in 1991. He received the B.S. and M.S. degree in material physics from the Harbin Institute of Technology, Harbin, China, in 2013 and 2015, respectively.

In 2015, he started his career as a Research Assistant with the Institute of Applied Electronics, China Academy of Engineering Physics, Mianyang, China. His research interests include design synthesis and fabrication of electromagnetic shielding materials and shielding effectiveness of materials under the excitation of high-intensity electromagnetic pulse.

FENG QIN was born in Huanggang, China, in 1985. He received the B.S. degree in applied physics from Shanghai Jiao Tong University, Shanghai, China, in 2007, and the Ph.D. degree in physics from The Chinese University of Hong Kong, Hong Kong, SAR, China, in 2016.

Since 2017, he has been an Associate Professor with the Institute of Applied Electronics, China Academy of Engineering Physics, Mianyang, China. He is the author of more than 30 articles, and more than 40 patents. His research interests include synthesis and characterization of electromagnetic shielding materials, complex electromagnetic environment effect, and electromagnetic hardening technology.

JINLIANG CAI was born in Changchun, China, in 1987. She received the Ph.D. degree from Jilin University, Changchun, China, in 2015. She is currently a Research Assistant with the Institute of Applied Electronics, China Academy of Engineering Physics, Mianyang, China. Her research interest includes electromagnetic pulse hardening technology.

SHOUHONG ZHONG was born in Zunyi, China, in 1993. He received the B.S. and M.S. degrees from Xidian University, Xi'an, China, in 2015 and 2018, respectively.

From 2018 to 2019, he worked with the Jiangnan Institute of Electrical and Mechanical Design, Guiyang, China. In 2019, he started his career as a Research Assistant with the Institute of Applied Electronics, China Academy of Engineering Physics, Mianyang, China. His research interests include electromagnetic protection circuit design and electromagnetic pulse effect.

JIANGCHUAN LIN was born in Mianyang, China, in 1984. He received the B.S. degree from Sichuan University, Chengdu, China, in 2006. Since 2019, he has been an Associate Professor with the Institute of Applied Electronics, China Academy of Engineering Physics, Mianyang. His research interests include complex electromagnetic environment effect and high-power microwave measurement.